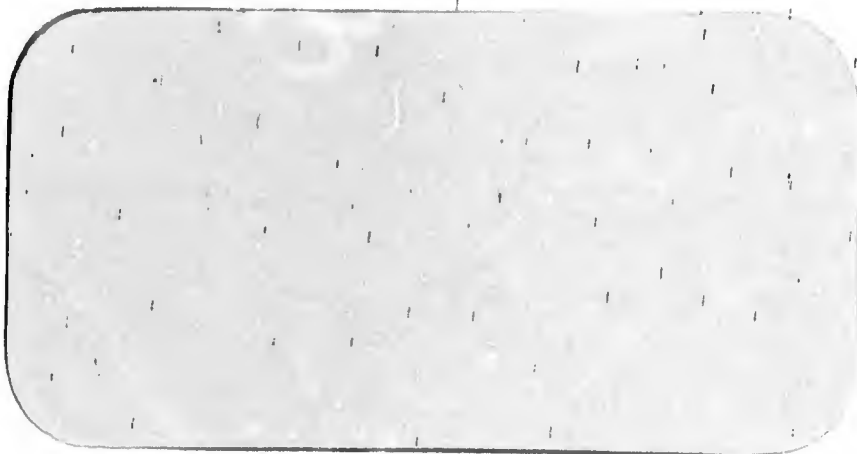


# IMS

## INSTITUTE OF MATERIALS SCIENCE

AD733369



F44620-69-C-0011

Reproduced by  
NATIONAL TECHNICAL  
INFORMATION SERVICE  
Springfield, Va. 22151

DDC  
RECEIVED  
DEC 7 1971  
C

"Approved for public release; distribution unlimited."

THE UNIVERSITY OF CONNECTICUT  
Storrs · Connecticut

25

UNCLASSIFIED

Security Classification

DOCUMENT CONTROL DATA - R & D

(Security classification of title, body of abstract and index annotation must be entered when the overall report is classified)

1. ORIGINATING ACTIVITY (Corporate author) UNIVERSITY OF CONNECTICUT DEPARTMENT OF METALLURGY STORRS, CONNECTICUT 06268	2a. REPORT SECURITY CLASSIFICATION UNCLASSIFIED
	2b. GROUP

3. REPORT TITLE  
CRACK OPENING DISPLACEMENT AND THE RATE OF FATIGUE CRACK GROWTH

4. DESCRIPTIVE NOTES (Type of report and inclusive dates)  
Scientific Interim

5. AUTHOR(S) (First name, middle initial, last name)  
RAYMOND J DONAHUE      HECTOR MCI CLARK      PHILLIP ATANMO      RAGHVIR KUMBLE  
ARTHUR J MCEVILY

5. REPORT DATE July 1971	7a. TOTAL NO. OF PAGES 26	7b. NO. OF REFS 39
-----------------------------	------------------------------	-----------------------

8a. CONTRACT OR GRANT NO. F44620-69-C-0011 8b. PROJECT NO. 7921 8c. 61102F 8d. 681307	9a. ORIGINATOR'S REPORT NUMBER(S) UC-MET-5-71
	9b. OTHER REPORT NO(S) (Any other numbers that may be assigned this report) AFOSR-TR-71-1946

10. DISTRIBUTION STATEMENT  
Approved for public release; distribution unlimited. *approximately equal to.*

11. SUPPLEMENTARY NOTES TECH, OTHER <i>20,000</i>	12. SPONSORING MILITARY ACTIVITY AF Office of Scientific Research (NAN) 1400 Wilson Boulevard Arlington, Virginia 22209
---	--

13. ABSTRACT  
Using a direct proportionality between the rate of fatigue crack growth and crack opening displacement above a threshold, it is shown that fatigue crack growth data for a wide variety of different materials can be accurately described in terms of the mechanical properties and two material constants; the constant of proportionality  $A$  and the threshold stress intensity factor  $K_{th}$ . Some 65 sets of data for tests at  $R = 0$  were analyzed by computer and it is shown that the approach is valid to growth rates up to about  $10^{-4}$  in./cycle, i.e. until the onset of crack propagation by dimple formation. It is found that  $A$  can be related to the yield strain for crack growth in non-aggressive environments, and is increased by increasingly severe environments, while  $K_{th}$  is decreased. These changes provide a measure of the severity of the environment. Crack growth rate in non-aggressive environments is shown to be independent of the yield stress and proportional to the strain intensity factor, above the threshold. The tabulation of  $A$  and  $K_{th}$  values as a function of material, environment and loading conditions provides a systematic engineering approach to estimating rates of fatigue crack growth and in determining the residual lifetimes of flawed structures.

*4*  
*K<sub>sub</sub>th*

DD FORM 1473 NOV 68

UNCLASSIFIED

Security Classification

UNCLASSIFIED

Security Classification

14. KEY WORDS	LINK A		LINK B		LINK C	
	ROLE	WT	ROLE	WT	ROLE	WT
CRACK OPENING DISPLACEMENT						
FATIGUE						
FATIGUE CRACK GROWTH						
ENVIRONMENTAL EFFECTS						
FRACTURE MECHANICS						

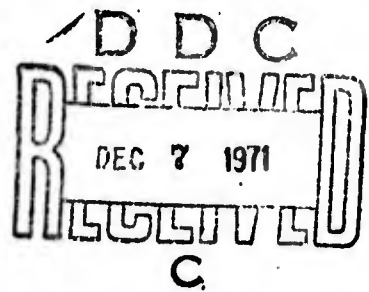
UNCLASSIFIED

CRACK OPENING DISPLACEMENT AND THE RATE OF FATIGUE CRACK GROWTH

by

R. J. Donahue,\* H. McI. Clark,\* P. Atanmo,\*\*

R. Kumble,\*\* and A. J. McEvily\*\*\*



\*Assistant Professor, Department of Metallurgy, University of Connecticut, Storrs, Connecticut.

\*\*Graduate Assistant, Department of Metallurgy, University of Connecticut, Storrs, Connecticut.

\*\*\*Professor and Head, Department of Metallurgy, University of Connecticut, Storrs, Connecticut.

## ABSTRACT

Using a direct proportionality between the rate of fatigue crack growth and crack opening displacement above a threshold, it is shown that fatigue crack growth data for a wide variety of different materials can be accurately described in terms of the mechanical properties and two material constants; the constant of proportionality  $A$  and the threshold stress intensity factor  $K_{th}$ . Some 65 sets of data for tests at  $R \approx 0$  were analysed by computer and it is shown that the approach is valid to growth rates up to about  $10^{-4}$  in./cycle, i.e. until the onset of crack propagation by dimple formation. It is found that  $A$  can be related to the yield strain for crack growth in non-aggressive environments, and is increased by increasingly severe environments, while  $K_{th}$  is decreased. These changes provide a measure of the severity of the environment. Crack growth rate in non-aggressive environments is shown to be independent of the yield stress and proportional to the strain intensity factor above the threshold. The tabulation of  $A$  and  $K_{th}$  values as a function of material, environment and loading conditions provides a systematic engineering approach to estimating rates of fatigue crack growth and in determining the residual lifetimes of flawed structures.

## CRACK OPENING DISPLACEMENT AND THE RATE OF FATIGUE CRACK GROWTH

INTRODUCTION. During the past decade the process of fatigue crack growth has been studied extensively and much data has been gathered. From time to time this data has been used to check various semi-empirical equations developed to relate stress state, crack length and material parameters to the rate of crack growth. One result of these studies is that the stress intensity factor has emerged as a useful unifying parameter. However, expressions which simply relate on an empirical basis the rate of crack growth to some power function of the stress intensity factor lack a mechanistic rationale and therefore obscure the role of material properties. In order to incorporate these into a crack growth expression consideration of the growth mechanism is necessary. One mechanism that has received wide support is the crack opening and closing or plastic blunting mode, Fig. 1 (1,2). This mechanism implies an increment of growth per cycle by a sliding off process during the tension stroke of the loading cycle. Such a model can be treated in terms of the crack opening displacement (COD) per cycle. If it is assumed that the amount of advance is proportional, to the COD, such a treatment leads to a second power dependence of the rate of crack growth on the stress intensity factor, as predicted by Liu (3) and McClintock (4) for example. Opinions have varied as to the applicability of a second power expression and the purpose of the present study is to reassess in a comprehensive fashion the general usefulness of a modified COD approach. To this end, some 65 sets of data on a variety of metals and alloys have been analyzed.

GENERAL APPROACH. Crack growth curves are usually presented as a plot of  $\log (\Delta a / \Delta N)$  with respect to  $\log K$ , where  $a$  is the crack length (or crack half-length for a centrally notched specimen),  $N$  the number of loading cycles and  $K$  the stress intensity factor, here defined as:

$$K = \sigma \sqrt{\alpha \pi a} \quad \dots\dots 1$$

where  $\sigma$  is the gross section stress and  $\alpha$  the finite width correction. Such a crack growth curve is shown schematically in Fig. 2. Because of the wealth of data for crack growth at  $R \approx 0$ , only this case is considered in the present paper. Analysis of the case  $R \neq 0$  will be the subject of a separate publication.

The form of the curve indicates that all crack growth rates fall within a range of stress intensity factor, bounded at the high  $K$  end by  $K_C$ , the fracture toughness, and at the low  $K$  end by a threshold value, here designated  $K_{th}$ . In contrast to the value of  $K_C$ , the value of  $K_{th}$  is very sensitive to the environment, since it has been well established that the position of  $K_{th}$  may be shifted to lower  $K$  values under the influence of an aggressive environment, (5). The lower bound means that a minimum value of the stress intensity factor is necessary for a crack to grow at all. The threshold concept has been incorporated in studies of fatigue crack growth notably that by McEvily and Illg (6,7) and more recently by Hartmann and Schijve (8) and by Paris (9). Any comprehensive analysis of fatigue crack growth must take into account the value of  $K_{th}$  and its shift with changing environment. An important consequence of the existence of a threshold is that it does not permit the description (10) of crack growth curves in their entirety in terms of a single overall slope.

At low stress intensity factors where the diameter of the plastic zone at the crack tip in a sheet specimen is much smaller than the specimen thickness, crack growth occurs under plane strain conditions, and the crack grows in the flat mode. At higher crack growth rates where the plastic zone is of the order of the specimen thickness a transition occurs to plane stress conditions, leading to slant fracture, and initially to a decrease in the crack growth rate, Fig. 2. The stress intensity factor at which this transition occurs will be a function of specimen thickness. In the slant mode crack growth does not occur primarily by striation formation but rather by a process of crack nucleation and dimple formation ahead of the main crack front (11), which quickly leads to a sharp increase in the rate of crack growth. This transition in fracture mode is observed to occur--for steels--at growth rates of about  $10^{-4}$  in./cycle (12). At growth rates above this value the idea of the COD applied to a single crack front is no longer applicable since crack growth then occurs additionally by tearing and dimple formation. It is expected that the present approach will be valid only at growth rates below about  $10^{-4}$  in./cycle.

We now proceed to the development of a modified COD expression for the rate of crack growth below  $10^{-4}$  in./cycle. It has been shown that K is related to COD of a stationary crack by the relationship, due to Wells (13):

$$\text{COD} = \frac{4K^2}{\pi\sigma_y E} \quad \dots 2$$

where  $\sigma_y$  is the yield stress of the material and E the Young's modulus.



A lower limiting value of K for crack growth thus implies a lower limiting value of COD for crack growth. If a direct interrelation of crack growth rate and COD of the type implied in Fig. 1 is assumed, then:

$$\frac{\Delta a}{\Delta N} = A[\text{COD} - (\text{COD})_{th}] \quad \dots 3$$

where  $(\text{COD})_{th}$  is the lower limiting value of the COD for crack growth and A is a dimensionless material constant of proportionality. Physically A reflects an assumed proportionality between the COD and the crack advance per cycle. It also incorporates any reversibility of the plastic blunting processes which may take place during unloading. The value of A will be much less than unity, based upon direct observation of the blunting process (14). However its assigned magnitude will of course reflect the particular numerical constants of Eq. 2.

Using Eq. 2 for the COD, Eq. 3 may be rewritten as:

$$\frac{\Delta a}{\Delta N} = \frac{4 A}{\pi \sigma_y E} [K^2 - K_{th}^2] \quad \dots 4$$

This equation expresses the rate of crack growth as a modified second power function of the stress intensity factor, through the incorporation of a threshold value below which crack growth does not occur. The material properties are reflected in the constants E,  $\sigma_y$ , A and  $K_{th}$ .

At gross section stresses where the crack tip plastic zone diameter becomes large, it is appropriate to apply a plastic zone correction to the crack length. This correction is made by taking the crack tip at the center of the plastic zone, Fig. 1, so that the left-hand side of Eq. 4 should be multiplied by the factor  $(1 - \frac{a^2 c^2}{2 \sigma_y^2})$ , (15). In anticipation of the results to be discussed later it may be said that this correction is not important in the present treatment and may be neglected.

METHOD OF ANALYSIS. The present study has been aimed at evaluating the usefulness of the approach expressed in Eq. 4 in describing the rate of growth of fatigue cracks in as wide a variety of metals and alloys as possible, using published crack growth data at  $R \approx 0$  and the mechanical properties of the material as input to determine the values of  $A$  and  $K_{th}$ .

Eq. 4 may be rearranged in log form:

$$\log \frac{\Delta a}{\Delta N} = \log \frac{4A}{\pi \sigma_y E} + \log (K^2 - K_{th}^2) \quad \dots 5$$

According to Eq. 5 a plot of  $\log \frac{\Delta a}{\Delta N}$  vs.  $\log (K^2 - K_{th}^2)$  should result in a straight line of slope 1. Based on this principle a computer program was written to obtain  $A$  and  $K_{th}$  values for as much slow crack growth data that allowed the overall slope of the plot to be  $1.00 \pm 0.05$ . A typical computer comparison for the data of Sallade and Clark (16) is shown in Fig. 3. From such a computer plot the upper limits of the validity of the expression can be noted at once. Typically those experimental points that diverge from the trend expected of Eq. 5 correspond to growth rates higher than  $10^{-4}$  in./cycle.

RESULTS AND DISCUSSION. The analysis of some 65 sets of data is summarized in Tables I - III. Table I gives data for aluminum alloys in all environments, Table II for steels in air and Table III for titanium and copper alloys. Included in each table is information on the material, the source of the data, yield stress, best fit values of  $A$  and  $K_{th}$  and the environment of the test as far as this was specified. Values for  $A$  and  $K_{th}$  have been assigned to every set of data, however, an adequate test of the method is only provided by those data collected over a wide range of crack growth rates, say  $10^{-7}$  to  $10^{-3}$  in./cycle. For growth rate ranges of only one or two orders of magnitude, a fit to Eq. 4 is of course easily obtained, but the values for  $A$  and  $K_{th}$  cannot be regarded as reliable. Those data that are felt to be particularly useful in

providing a critical test of the approach, and thus give reliable values of  $A$  and  $K_{th}$ , are indicated with an asterisk in the tables. Examples of the comparison of crack growth data and the best fit from Eq. 4 for an aluminum alloy (6), a titanium alloys (16) and a steel (12) are shown in Figs. 4, 5 and 6 respectively. The fit is excellent up to a growth rate of about  $10^{-4}$  in./cycle, deviation occurring at higher rates for which Eq. 4 is not expected to be valid. Crack growth rates above  $10^{-4}$  in./cycle may be accounted for by assuming a linear relationship between logarithm of growth rate and the stress intensity factor (6,7), by incorporating a rapid but finite crack growth rate corresponding with  $K_c$ , the fracture toughness(39).

By definition  $K_{th}$  is the threshold stress intensity factor. Values for steels, Table II, range from 12.4 to 63.5  $\text{ksi}\sqrt{\text{in.}}$ . We do not feel confident about the correctness of all of these values since the computer program tended to define a threshold rather close to the lowest crack growth rate point, so that some of the  $K_{th}$  values are undoubtedly unrealistically high. These values have been enclosed by parentheses in Tables 1-3. This uncertainty would be greatly reduced by measurements down to about  $10^{-7}$  in./cycle since the downward curve of points to the threshold should then become apparent. However, examination of all  $K_{th}$  values in Tables I-III reveals a trend for increasing  $K_{th}$  with increasing Young's modulus; e. g. steels show values of about 17  $\text{ksi}\sqrt{\text{in.}}$ , while aluminum alloys have values of about 5  $\text{ksi}\sqrt{\text{in.}}$ , in the absence of environmental effects.

The parameter  $A$  in Eq. 4 relates the crack growth rate/cycle to the COD/cycle above the threshold. In the absence of environmental effects  $A$  has a value of about 0.01, implying that the crack advance is about 1% of the COD above the threshold. It is particularly interesting to note that  $A$  can be related to the yield strain,  $\sigma_y/E$ . A plot of  $A$ , for non-aggressive environments, with respect to  $2\sigma_y/E$  gives a straight line of slope 1, Fig. 7.

This implies that a value for A in Eq. 4 for crack growth in vacuum can be calculated from a knowledge of  $\sigma_y$  and E only.

The dependence of A upon the yield strain suggests that the advance per cycle is dependent upon the strain hardening rate, since in general it is to be expected that the higher the ratio of yield stress to modulus, the lower will be the rate of strain hardening. This finding is in accord with the expectation that an increase in strain hardening rate will increase the ratio of COD to the crack advance per cycle, (14).

As shown by the values listed in Tables I-III, for inert environments the value of  $AE/2\sigma_y$  may be taken to be unity. We shall presently discuss the effect of an aggressive environment on the value of A, but it should be noted that other factors can lead to  $AE/2\sigma_y$  values other than unity. In Table II the data of Brothers and Yukawa (31) and Crooker et al. (32) may be compared with that of Greenberg et al. (28) and Wessell et al. (29) respectively. The former authors' data yield values from 1.8 to 4.1, while data from the latter authors for the same steels give values of about unity. We believe that this discrepancy arises from the fact that data of Brothers and Yukawa and Crooker et al. were taken at relatively high growth rates, from  $10^{-5}$  to  $10^{-3}$  in./cycle, in which range the present approach becomes invalid. Thus, although a computer fit of these data was obtained--giving values of A and  $K_{th}$ --these values are almost certainly too high.

Upon substituting  $2\sigma_y/E$  for A in Eq. 4 we obtain:

$$\frac{\Delta a}{\Delta N} = \frac{8}{\pi} \left[ \frac{K^2}{E^2} - \frac{K_{th}^2}{E^2} \right] \quad \dots 6$$

where  $K/E$  is the strain intensity factor (37). It is seen that crack growth rate depends on the square of the strain intensity factor and that a dominant material parameter affecting crack growth is Young's modulus. The yield stress

does not explicitly appear in this equation, however it should be kept in mind that this equation is only valid for net section stresses well below yield.

A number of other investigators, (12, 17, 37) have shown that crack growth rate where the environment is not a factor should be independent of the yield stress, and of the form:

$$\frac{\Delta a}{\Delta N} = (\text{Const.}) \frac{K^2}{E^2} \quad \dots 7$$

Such a relationship can only be valid where the threshold is no longer important, and is readily deduced from Eq. 6. It is of interest to note that the study of Clark and Bates (17) based on striation spacing, of Barsom et al. (12) on steels, of Hahn et al. (37) for a number of alloys at a constant crack growth rate of  $10^{-5}$  in./cycle, and the present investigation for the range in which it is valid all yield the same constant of proportionality in Eq. 7.

An evaluation of the effect of environment on A and  $K_{th}$  is possible by comparing results on crack growth in vacuum with results on the same material in an aggressive environment. Analysis of the results obtained by Bradshaw and Wheeler (24) listed in Table I shows that in vacuum the aluminum alloy 5070A (equivalent to 2024-T3) has a value of A of 0.01 and the parameter  $AE/2\sigma_y$  a value of 0.9. The same result obtains for tests in nitrogen and oxygen atmospheres of low water content, so that it may be concluded that these environments are neutral for this material. On testing in air the A value is 0.019 and  $AE/2\sigma_y$  1.75, while in water A is 0.033 and  $AE/2\sigma_y$  3.0. Three different investigations of crack growth in 2024-T3

aluminum in air give A values of 0.02 and  $AE/2\sigma_y$  values of 2.1. The shift of  $K_{th}$  to lower stress intensity factor values is shown by the same results, changing from about 5 in an inert environment to about 3.5 in aggressive environments.

The same pattern is shown by Bradshaw and Wheeler's results (24) for aluminum alloy 683 (comparable with 7075-T6) for which A values rise by a factor of about 9 from vacuum to water, while the  $K_{th}$  values fall from 6.5 to 3.5. For a given material in different environments, the rates of crack growth relative to that in vacuum are given by the ratio of A in an environment to A in vacuum which equals  $AE/2\sigma_y$ , at stress intensity values remote from the threshold. Thus for 5070A tested in water ( $AE/2\sigma_y = 3$ ) the growth rate is three times faster than in vacuum, where the threshold stress intensity factor is no longer important, Fig. 6. Insufficient information on crack growth in vacuum and in various environments for alloys other than aluminum does not allow confirmation of these conclusions for other materials. However, from the evidence presently available it is to be expected that increasingly aggressive environments will cause A to increase and  $K_{th}$  to decrease. Physically this means that a crack will propagate at a lower stress intensity factor than is possible in vacuum (lower  $K_{th}$ ) and that the advance per cycle increases for a given stress intensity factor, a likely result of surface chemical reaction.

SUMMARY AND CONCLUSIONS. Using a direct relationship between crack opening displacement above a threshold value and the rate of fatigue crack growth  $\Delta a/\Delta N$  it has been shown that fatigue crack growth data for a wide variety of different materials can be accurately described in terms of the mechanical properties of the material and two material constants A and  $K_{th}$  in the equation:

$$\frac{\Delta a}{\Delta N} = \frac{4 A}{\pi E \sigma_y} [K^2 - K_{th}^2]$$

This relationship has been found to be valid up to crack growth rates of about  $10^{-4}$  in./cycle, i.e. up to the onset of rupture by dimple formation. The constant A is found to be proportional to the yield strain,  $\sigma_y/E$ , in non-aggressive environments, but increases with increasing severity of the environment. For a given specimen tested in an aggressive environment the parameter  $AE/2\sigma_y$  gives a direct measure of the crack growth rate with respect to a specimen tested under the same conditions in a non-aggressive environment. Most of the data concerning the threshold stress intensity value has been obtained for aluminum alloys, and for these alloys it is seen that the  $K_{th}$  is highest in vacuum and decreases with increasing aggressiveness of the environment. Although sufficient data are lacking for other alloy systems, it is expected that this trend will be followed for these materials also. At values of the stress intensity factor where the effect of the threshold can be neglected the crack growth rate is directly proportional to the stress intensity factor  $K^2/E^2$ .

It is concluded that the crack opening displacement concept is successful in describing fatigue crack growth data up to the onset of fracture by tearing dimple formation. Further, the tabulation of A and  $K_{th}$  values as a function of material, environment and loading conditions should provide a useful systematic engineering approach to estimating rates of fatigue crack growth and in determining residual lifetimes of flawed structures.

1. C. Laird, Fatigue Crack Propagation, ASTM STP 415 (1967).
2. J. E. Srawley, J. L. Swedlow and E. Roberts, Jr., Int. Journ. of Fracture Mech., Vol. 6, p. 441 (1970)
3. H. W. Liu, Fatigue: An Interdisciplinary Approach, Syracuse University Press (1964).
4. F. A. McClintock, Fatigue Crack Propagation, ASTM STP 415 (1967)
5. F. J. Bradshaw and C. Wheeler, RAE Tech. Report No. 65073 (April, 1965)
6. A. J. McEvily and W. Illg, "The Rate of Crack Propagation in Two Aluminum Alloys," NACA TN 4394 (September, 1958).
7. A. J. McEvily and W. Illg, "An Investigation of Non-propagating Fatigue Cracks," NASA TN D-208, 1959.
8. A. Hartman and J. Schijve, "The Effects of Environment and Load Frequency on the Crack Propagation Law for Macro Fatigue Crack Growth in Aluminum Alloys", NLR MP 68001 U, National Aerospace Laboratory, NLR, The Netherlands.
9. P. C. Paris, Professor of Mechanics, Lehigh University, Bethlehem, Pa., private communication.
10. P. C. Paris, Fatigue: An Interdisciplinary Approach, Syracuse University Press (1964).
11. R. W. Hertzberg, Fatigue Crack Propagation, ASTM STP 415 (1967).
12. J. M. Barsom, E. J. Imhof, and S. T. Rolfe, "Fatigue-Crack Propagation in High Yield-Strength Steels," submitted to J. Eng. Fract. Mech.
13. A. A. Wells, Proc. Crack Propagation Symposium, Cranfield (1961).
14. A. J. McEvily and T. L. Johnston, "The Role of Cross Slip in Brittle Fracture and Fatigue, International Conference on Fracture, Sendai, Japan, Sept. 12-17, 1965.
15. D. P. Rooke, Ministry of Technology, Royal Aircraft Establishment, private Communication.
16. P. L. Sallade and H. McI. Clark, Dept. of Metallurgy, Univ. of Conn., Storrs, (to be published).
17. W. G. Clark, Jr. and R. C. Bates, Westinghouse Research Lab. Scientific Paper 69-1E7-RDAFC-P1 (Dec. 4, 1969).
18. R. G. Forman, V. E. Kerney and R. M. Engle, "Numerical Analysis of Crack Propagation in Cyclic Loaded Structures," Trans. ASME, 89B (September, 1967).



19. C. M. Hudson and H. F. Hardrath, "Effects of Changing Stress Amplitude on the Rate of Fatigue Crack Propagation in Two Aluminum Alloys," NASA TN D-960 (September, 1961).
20. C. M. Hudson and J. T. Scardina, "Effect of Stress Ratio on Fatigue-Crack Growth in 7075-T6 Aluminum Alloy Sheet," NASA TN D-5390 (August 1969).
21. D. Broek and J. Schijve, "The Influence of the Mean Stress on the Propagation of Fatigue Cracks in Aluminum Alloy Sheet," Nat. Aero. Res. Inst. (Amsterdam), Report NLR-TN M.2111 (January 1963).
22. R. P. Wei and J. D. Landes, *Int. J. Fracture Mech.*, Vol. 5, p. 69 (1969).
23. W. G. Fleck and R. B. Anderson, *Proc. 2-d Int. Conf. on Fatigue*, Brighton (April 1969).
24. F. J. Bradshaw and C. Wheeler, *Int. J. Fracture Mech.*, Vol. 5, p. 255 (1969).
25. D. R. Donaldson and W. E. Anderson, *Proceedings of Crack Propagation Symposium*, College of Aero, Cranfield, England, pp. 375-441 (September 1961).
26. C. M. Carman and J. M. Katlin, "Low Cycle Fatigue Crack Propagation of High Strength Steels," *ASME 66-MET-3* (April 1966).
27. W. G. Clark, Jr., *Engineering Fracture Mech.*, Vol. 1, p. 385, (1968).
28. H. D. Greenberg, E. T. Wessel, W. G. Clark, Jr., and W. H. Pryle, *Westinghouse Research Lab. Scientific*, Paper 69-1D9-MEMTL-P1 (October 1969).
29. E. T. Wessel, W. G. Clark, Jr., and W. K. Wilson, *Westinghouse Research Lab. Final Tech. Report Contract No. DA-30-069-AMC-602 (T)*, (June 24, 1966).
30. G. A. Miller, *Trans. ASM*, Vol. 61, p. 442 (1968).
31. A. J. Brothers and S. Yukawa, *Trans. ASME*, p. 19 (march 1967).
32. T. W. Crooker, L. A. Cooley, E. A. Lange and C. N. Freed, *Trans. ASM*, Vol. 61, p. 568 (1968).
33. R. J. Bucci, *Thesis (Lehigh University)*, (1970).
34. R. G. Kimble and A. J. McEvily, *Dept. of Metallurgy, Univ. of Conn., Storrs*, Private communication.
35. A. J. McEvily, Jr., and R. C. Boettner, *Acta Met.*, Vol. 11, p. 725, (1963).
36. A. J. McEvily, Jr., *Proc. Conf. on Fatigue and Fracture of Aircraft Structures and Materials*, AFFDL TR70-144, pp. 451, (1970).
37. G. T. Hahn, A. R. Rosenfield and M. Sarrate, *Wright-Patterson Tech. Report AFML-TR-67-143* (September 1969).
38. D. A. Meyn, *Metallurgical Trans.* (to be published).
39. A. J. McEvily, Jr. and R. Kumble (to be published).

## FIGURE CAPTIONS

- Fig. 1. Schematic diagram of the fatigue crack growth process showing the interrelationship of crack opening displacement (COD) and crack advance per cycle  $\left(\frac{\Delta a}{\Delta N}\right)$ , after (1).
- Fig. 2. Schematic plot of crack growth rate per cycle  $\left(\frac{\Delta a}{\Delta N}\right)$  with respect to log (stress intensity factor) showing the upper and lower limits of stress intensity factor,  $K_c$  and  $K_{th}$ .
- Fig. 3. Computer plot of Eqn. 7 of data for Ti-6Al-4V from (16) showing excellent fit up to a crack growth rate of  $10^{-4}$  in./cycle.
- Fig. 4. Comparison of calculated best fit curve and experimental crack growth data for 2024-T3 aluminum from (6).
- Fig. 5. Comparison of calculated best fit curve and experimental crack growth data for Ti-6Al-4V from (16).
- Fig. 6. Comparison of calculated best fit curve and experimental crack growth data for 10Ni-Cr-Mo-Co steel from (12).
- Fig. 7. Plot of the proportionality constant  $A$  with respect to twice the yield strain  $\left(\frac{2\sigma_y}{E}\right)$  for a variety of materials in non-aggressive environments.
- Fig. 8. Crack growth data for aluminum alloy 5070A in various environments from the work of Bradshaw & Wheeler (24).

TABLE 1

Values of parameters in Eqn. 4 calculated from crack growth data for  
Aluminum Alloys

<u>MATERIAL</u>	<u>REFERENCE</u>	<u>Y.S.</u> <u>ksi</u>	<u>A</u>	$K_{th}$ <u>ksi<math>\sqrt{in.}</math></u>	$\frac{AE}{2\sigma_y}$	<u>ENVIRONMENT</u>
7079-T6	Clark & Bates (17)	65	0.012	12.2	0.95	Air (Striation spacing)
* 7075-T6	McEvily & Illg (6) Forman et al. (18) Hudson & Hardrath (19) Hudson & Scardina (20) Broek & Schijve (21)	70	0.05	4.7	3.75	Air
7075-T651	Wei & Landes (22)	70	0.035 0.115	8.1 5.5	2.65 8.7	Argon H <sub>2</sub> O or D <sub>2</sub> O
6061-T6	Fleck & Anderson (23)	43	0.008	8.6	1.0	Air
5456-H321	Clark & Bates (17)	37	0.0058	5.7	0.85	Air (striation spacing)
* 5070A	Bradshaw & Wheeler (24)	58	0.01 0.01 0.01 0.019 0.033	5.8 5.1 4.8 3.7 4.3	0.9 0.9 0.9 1.75 3.0	Vacuum N <sub>2</sub> (H <sub>2</sub> O 8 Nm <sup>-2</sup> ) O <sub>2</sub> (H <sub>2</sub> O 1 Nm <sup>-2</sup> ) Air Water
*683	Bradshaw & Wheeler (24)	77	0.015 0.015 0.05 0.13	6.5 6.5 2.8 4.3	1.05 1.05 3.5 9	Vacuum N <sub>2</sub> (H <sub>2</sub> O 7 Nm <sup>-2</sup> ) Air Water
* 2024-T3	McEvily & Illg (6) Donaldson & Anderson (25) Hudson & Hardrath (19)	51	0.02	5.0	2.7	Air
Al-2.2Cu-1.6Mg	Bradshaw & Wheeler (5)	40	0.01 0.03	5.3 4.1	1.35 4.0	Vacuum Air

\* Considered reliable (See Text)

( ) Unrealistically high

TABLE II

Values of parameters in Eqn. 4 calculated from crack growth data for  
Steels

<u>MATERIAL</u>	<u>REFERENCE</u>	<u>Y.S.</u> <u>ksi</u>	<u>A</u>	$K_{th}$ <u>ksi<math>\sqrt{in.}</math></u>	$\frac{AE}{2\sigma_y}$	<u>ENVIRONMENT</u>
* HY-80	Barsom et al. (12)	95	0.006	24.8	0.95	Air
* HY-130		140	0.011	16.8	1.2	"
* 10Ni-Cr-Mo-Co		191	0.014	11.1	1.15	"
* 12Ni-5Cr-3Mo		185	0.013	18.6	1.05	"
18Ni (250)	Carmen & Katlin (26)	252	0.016	14.2	0.95	"
18Ni (300)		295	0.025	21.6	1.3	"
* Ni-Mo-V	Clark (27)	84	0.005	30.0	0.9	"
Ni-Mo-V	Greenberg et al. (28)	74	0.0055	(35.0)	1.1	"
Cr-Mo-V		94	0.006	(62.0)	1.0	"
Ni-Cr-Mo-V		156	0.009	(47.5)	0.9	"
HP-9-4-25	Wessel et al. (29) Clark & Bates (17) Clark (27)	175	0.014	29.6	1.2	"
A533	Clark & Bates (17)	73	0.005	(35.4)	1.0	"
4330 (1000)	Miller (30)	163	0.029	16.6	2.7	"
18Ni (900)		245	0.055	12.6	3.3	"
18Ni (1100)		218	0.066	12.4	4.5	"
4340 (1400)		63	0.02	20.0	4.8	"
4340 (500)		222	0.1	15.8	6.5	"
4340 (200)		193	0.19	17.7	14.0	"
H-11 (950)		208	0.27	19.5	16.0	"
Cr-Mo-V	Brothers & Yukawa (31)	100	0.014	(68.4)	2.0	"
		127	0.015	(63.5)	1.8	"
		85	0.015	(62.9)	2.5	"
Ni-Cr-Mo-V		117	0.016	(39.3)	2.0	"
		84	0.015	(45.8)	2.5	"
		73	0.016	(51.7)	3.0	"
HP-9-4-25	Crooker et al. (32)	183	0.05	(40.7)	4.1	"

\*Considered reliable (See Text)

( ) Unrealistically high

TABLE III

Values of Parameters in Eqn. 4 calculated from crack growth data for  
Titanium and Copper Alloys

<u>MATERIAL</u>	<u>REFERENCE</u>	<u>Y.S.</u>	<u>A</u>	$\frac{K_{th}}{ksi\sqrt{In.}}$	$\frac{AE}{2\sigma_y}$	<u>ENVIRONMENT</u>
* Ti-6Al-4V	Clark & Bates (17)	120	0.014	(21.2)	0.95	Air (striation spacing)
	Sallade & Clark (16)	141	0.036	6.7	2.4	Air (80°F)
		91	0.020	6.2	1.57	" (550°F)
		70	0.016	3.9	1.6	" (850°F)
		35	0.014	2.5	2.75	" (1150°F)
Ti-5Al-2.5Sn	Fleck & Anderson (23)		0.022	5.3	4.45	"
* Ti-8Al-1Mo-1V	Bucci (33)	135	0.016	17.7	0.95	Argon, 5 cps
			0.03	19.5	1.75	" 0.5 cps
			0.037	10.8	2.15	3.5%NaCl, 50 cps
			0.045	10.6	2.65	" 5 cps
			0.052	15.0	3.05	" 0.5 cps
	Meyn (38)	136	0.018	14.2	1.0	Vacuum 20-30 cps
			0.032	8.9	1.85	Air 20-30 cps
* OFHC-Cu	Kumble & McEvily (34)	12	0.0015	3.7	1.05	Air
* Cu-5.6Al	McEvily (35)	18.9	0.002	6.4	0.95	"
* Cu-6.5Al-2.4Fe		32.8	0.004	7.1	1.1	"
* Cu-30Zn (Ann.)		18	0.002	6.7	0.95	"
* Cu-30Zn (.W.)		92	0.019	6.7	1.65	"

\*Considered reliable (See Text)

( ) Unrealistically high

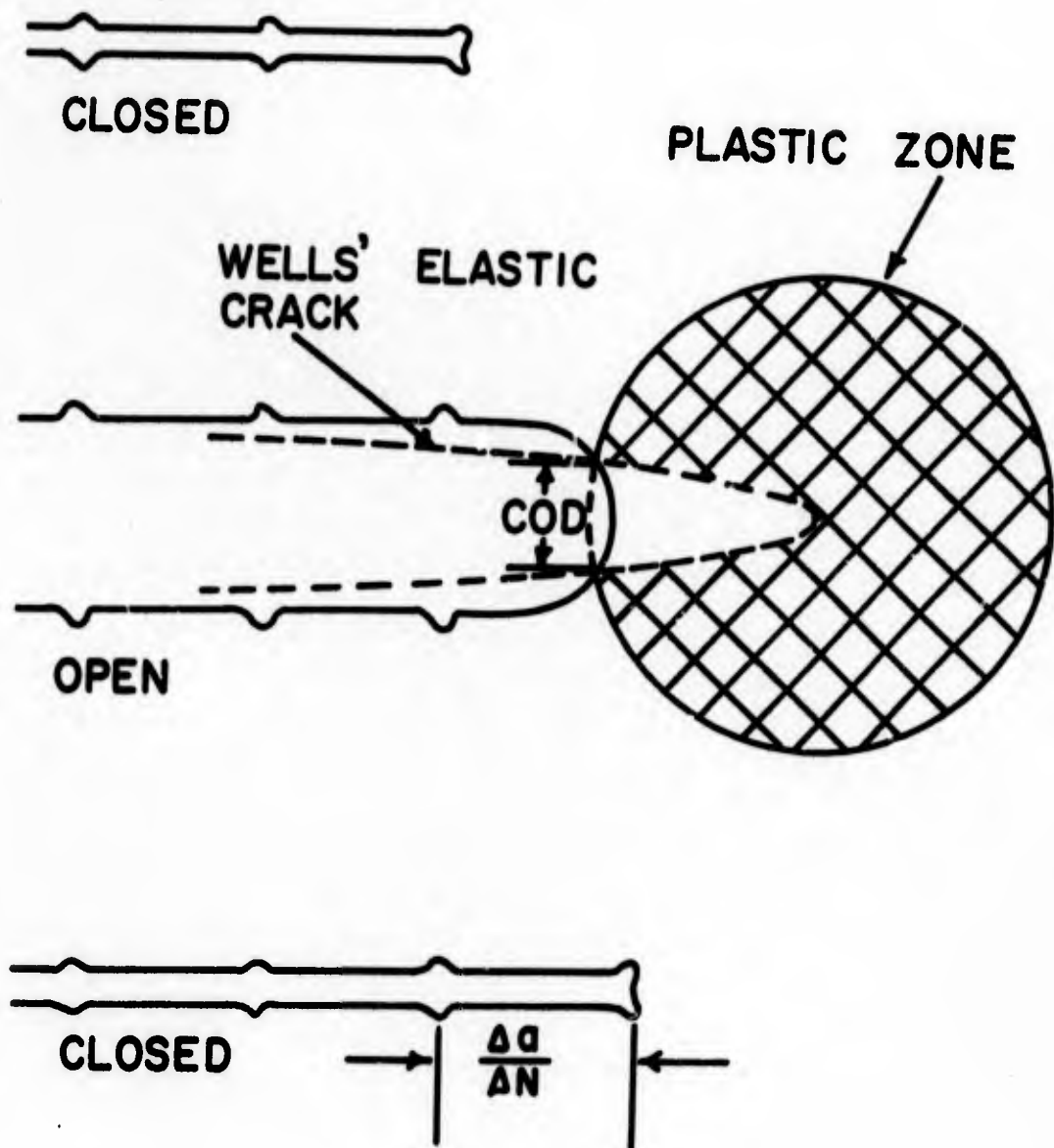


Fig. 1

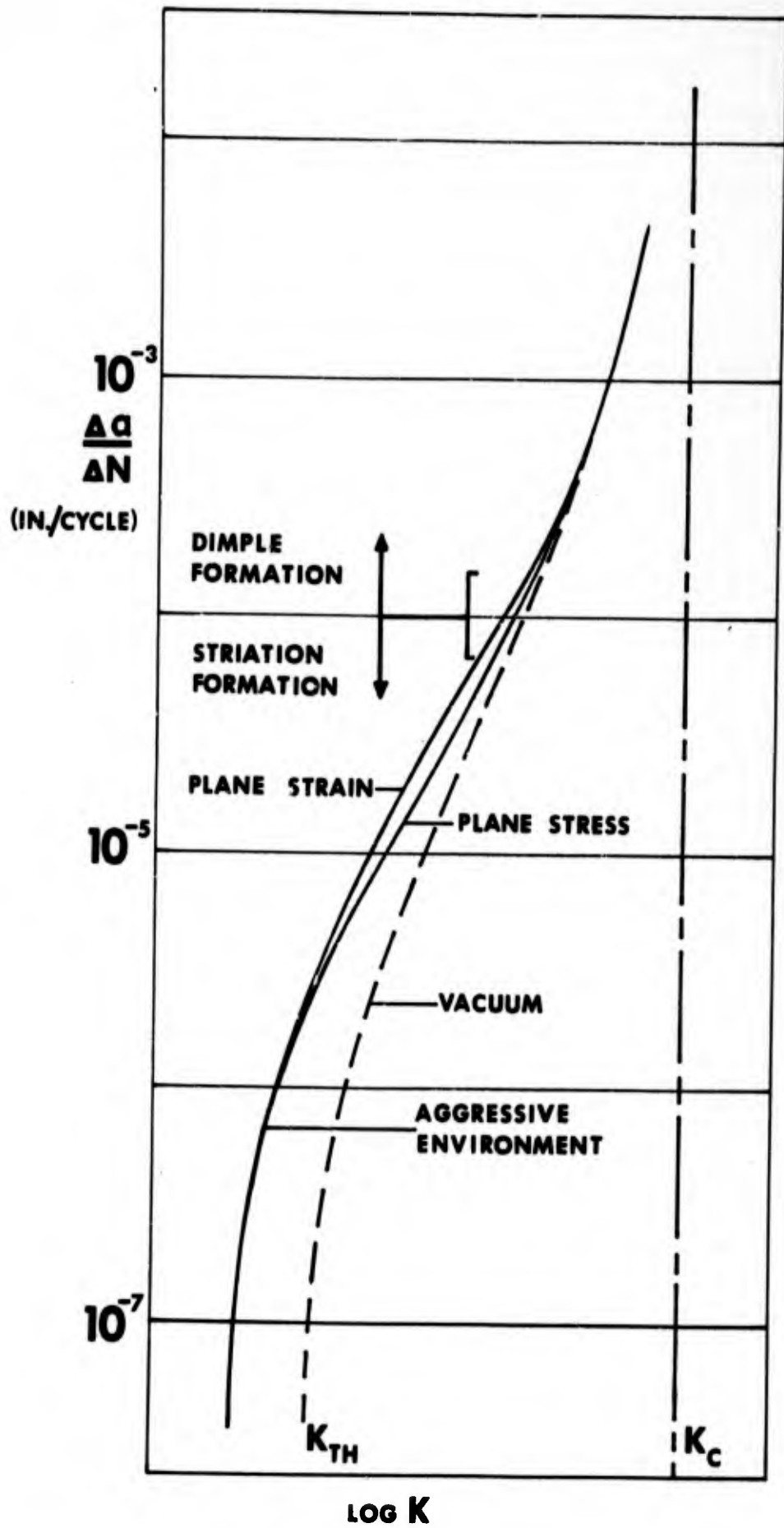


Fig.2

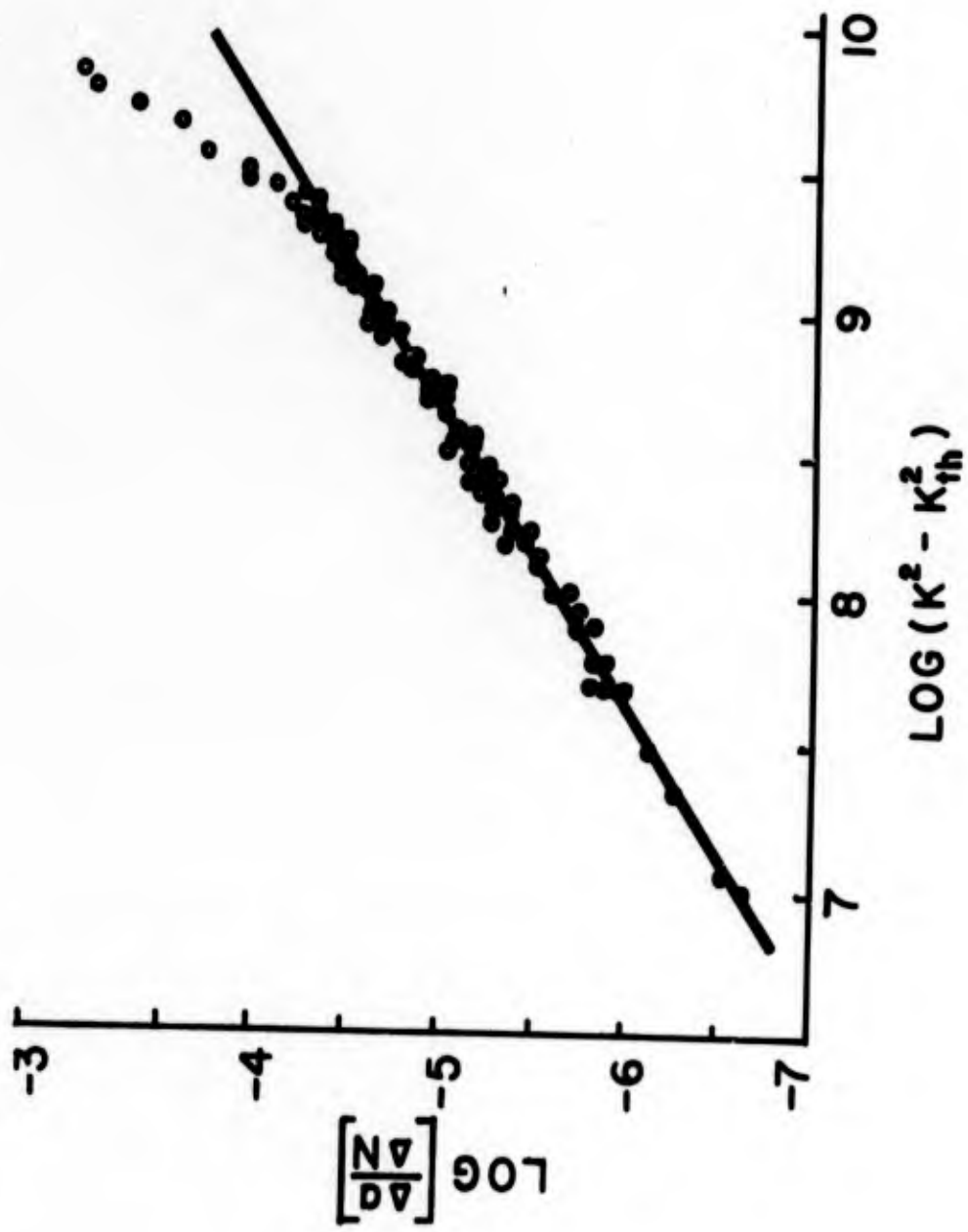


Fig. 3



2024 - T3 ALUMINUM

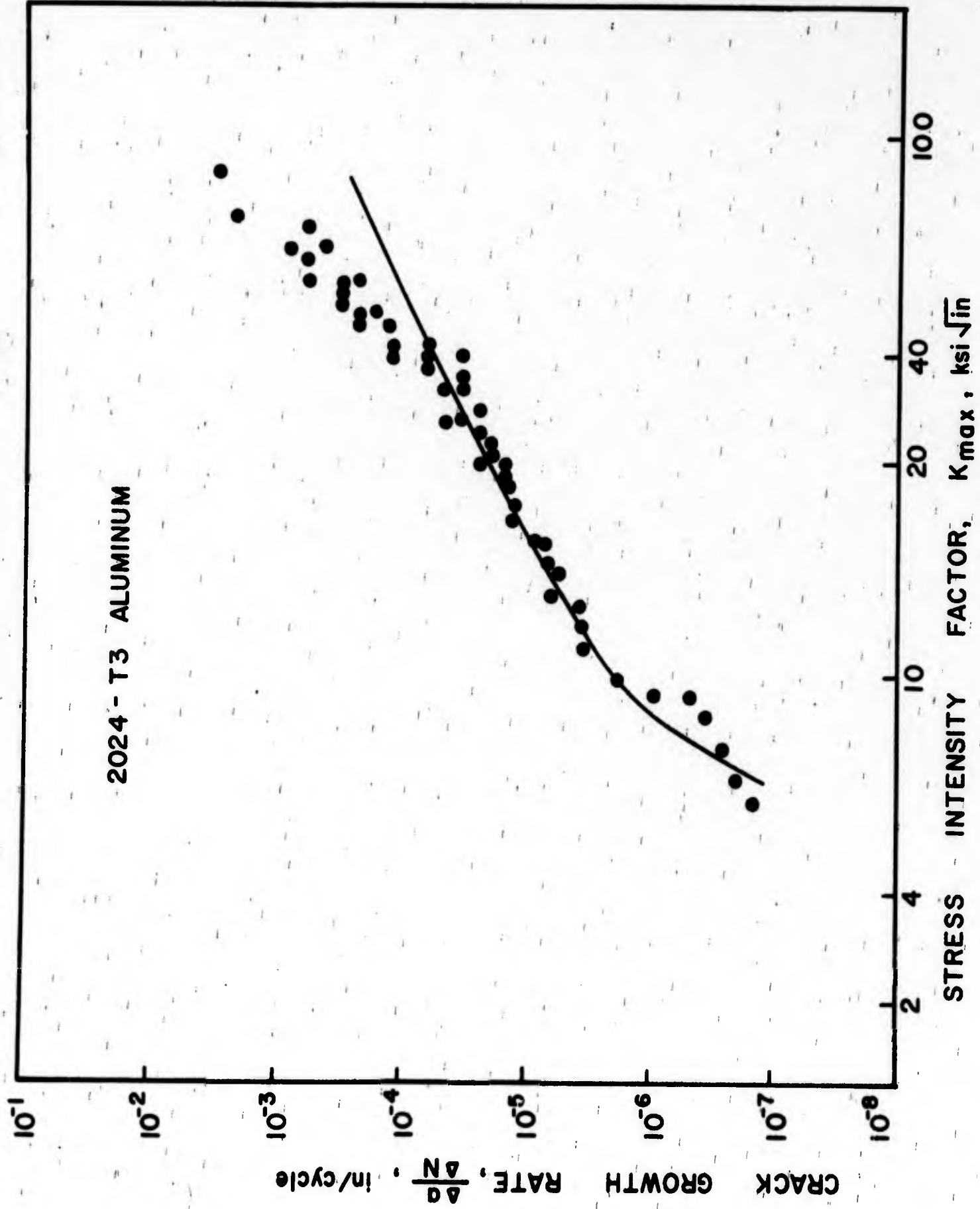
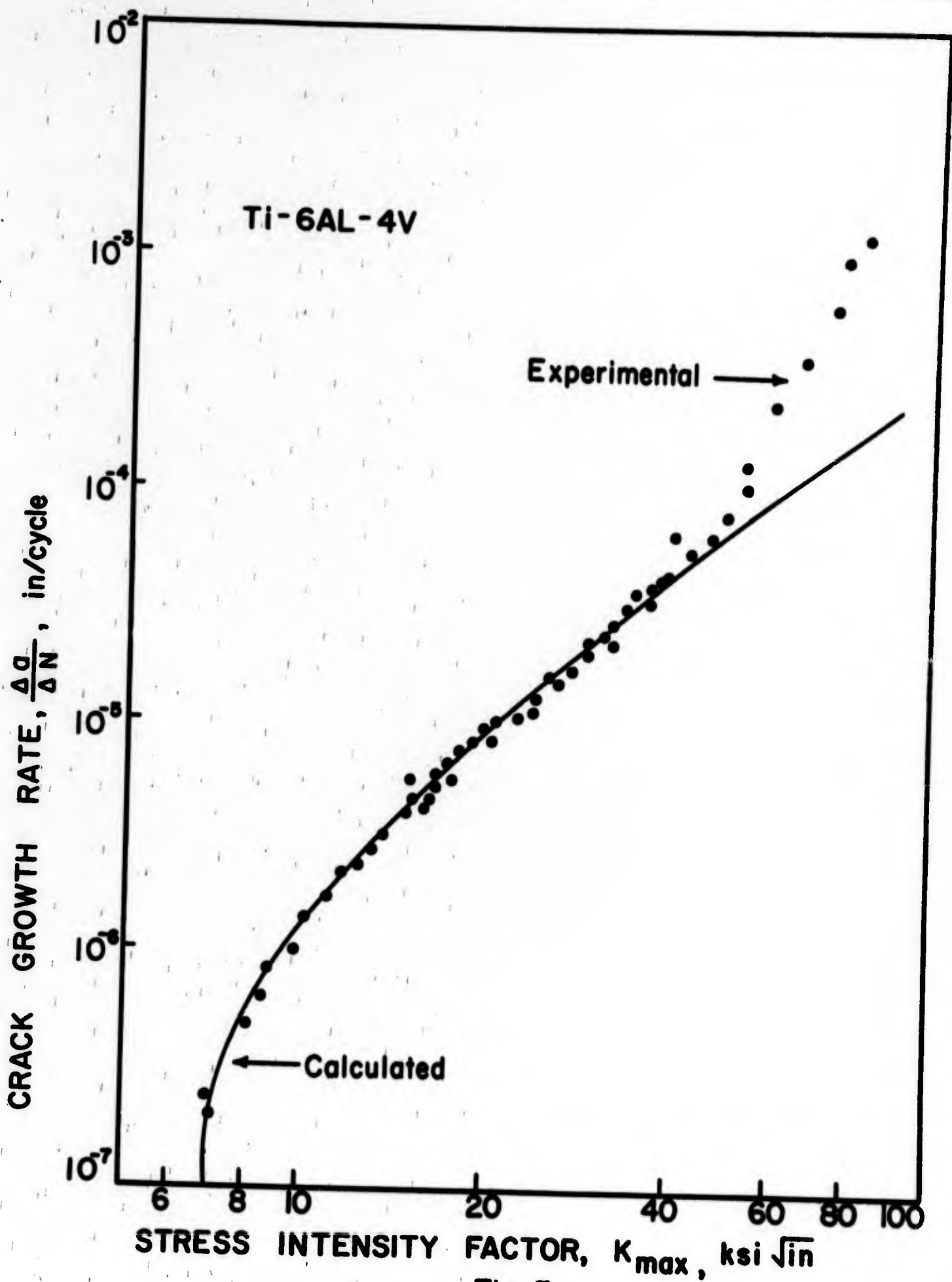


Fig. 4



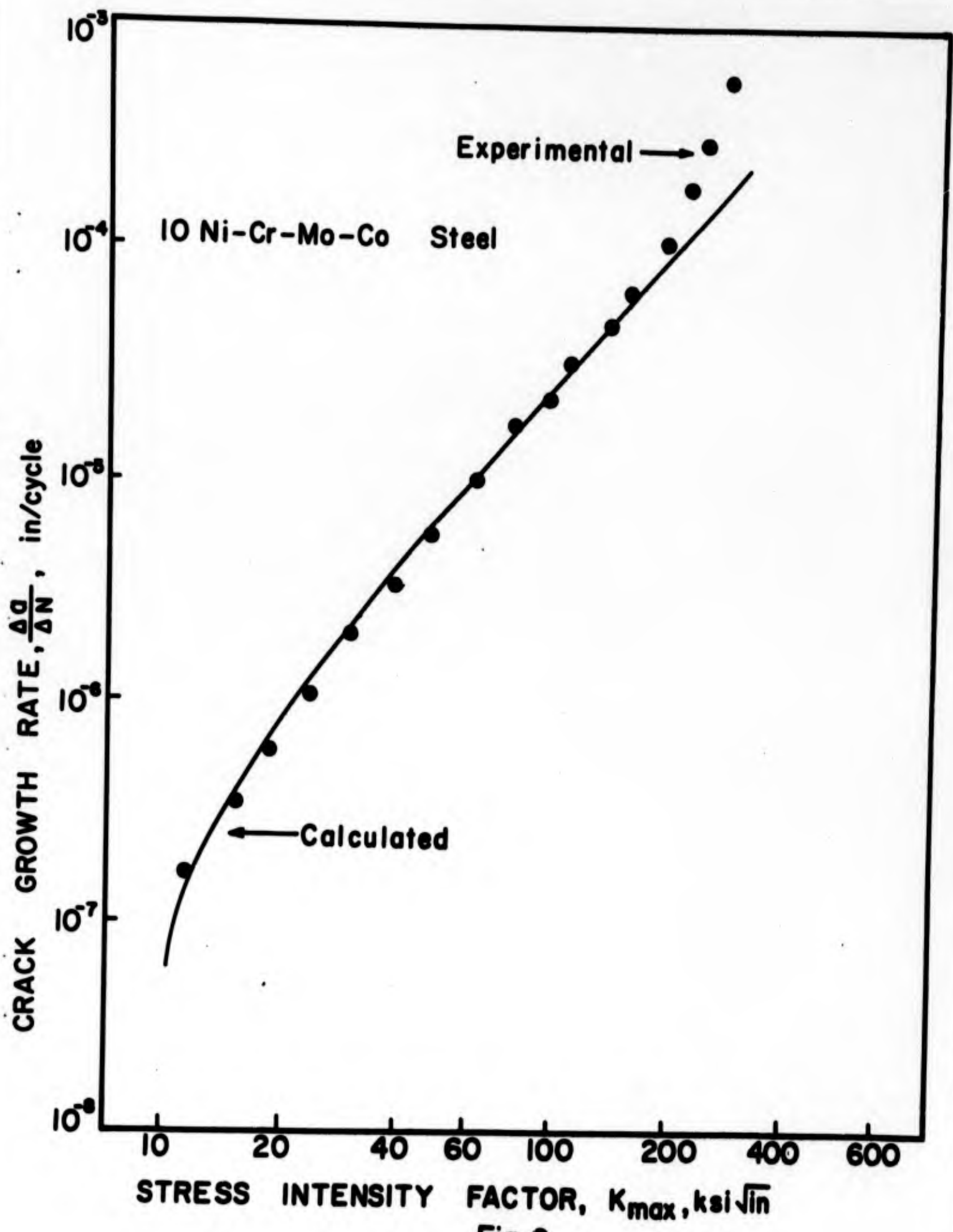


Fig. 6

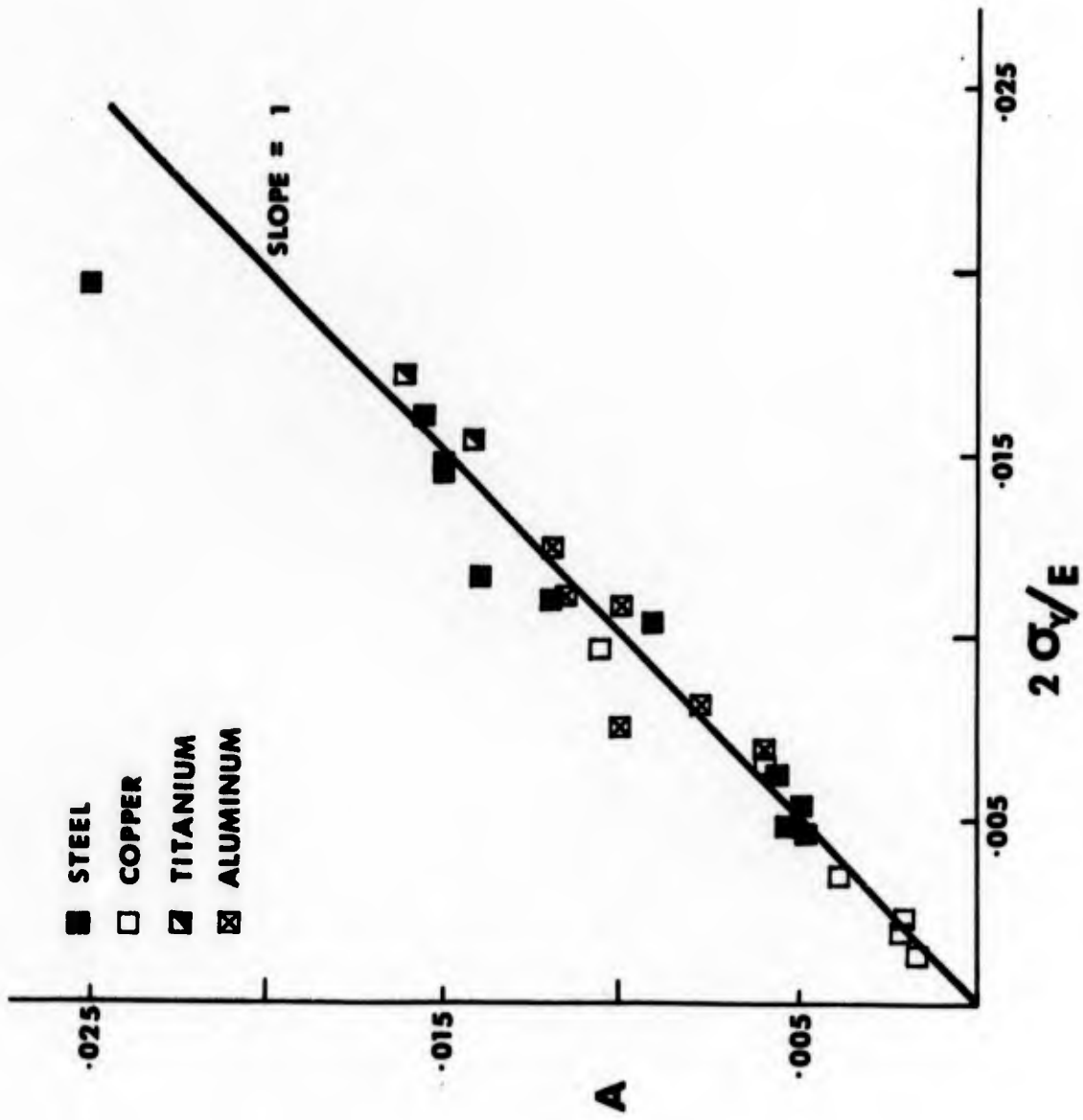


Fig. 7

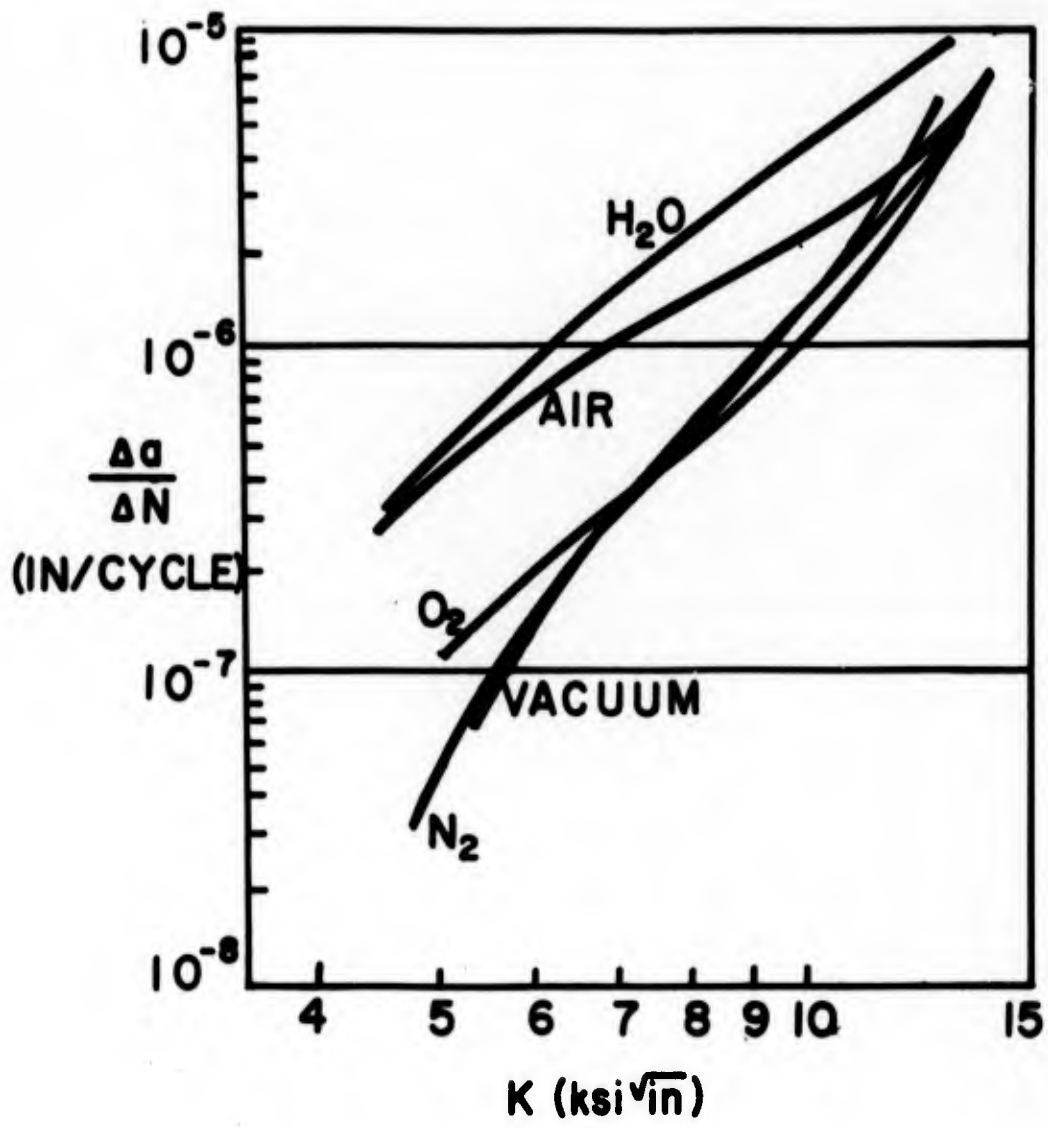


Fig. 8